Hindawi Publishing Corporation
Journal of Nanotechnology
Volume 2015, Article ID 350370, 10 pages
http://dx.doi.org/10.1155/2015/350370

Research Article

Synthesis, Characterization, and *In Vitro* Drug Delivery Capabilities of (Zn, Al)-Based Layered Double Hydroxide Nanoparticles

Vinay J. Nagaraj,[1] Xiaodi Sun,[2] Jiten Mehta,[1] Mac Martin,[1] Thi Ngo,[1] and Sandwip K. Dey[2]

[1]*Department of Biochemistry, Midwestern University, Glendale, AZ 85308, USA*
[2]*School for Engineering of Matter Transport and Energy, Arizona State University, Tempe, AZ 85287, USA*

Correspondence should be addressed to Vinay J. Nagaraj; nvinay@midwestern.edu and Sandwip K. Dey; sandwip.dey@asu.edu

Received 26 June 2015; Revised 21 September 2015; Accepted 27 September 2015

Academic Editor: Su Seong Lee

Copyright © 2015 Vinay J. Nagaraj et al. This is an open access article distributed under the Creative Commons Attribution License, which permits unrestricted use, distribution, and reproduction in any medium, provided the original work is properly cited.

There is an urgent need for the development of alternative strategies for effective drug delivery to improve the outcome of patients suffering from deadly diseases such as cancer. Nanoparticles, in particular layered double hydroxide (LDH) nanoparticles, have great potential as nanocarriers of chemotherapeutic molecules. In this study, we synthesized (Zn, Al)-LDH nanoparticles and report their enhanced pH-dependent stability in comparison to the commonly used (Mg, Al)-LDH nanoparticles. Fluorescein isothiocyanate (FITC) and valproate (VP) were intercalated into (Zn, Al)-LDH nanoparticles to study cellular uptake, biocompatibility, and drug delivery capabilities using cultured pancreatic adenocarcinoma BxPC3 cells. Fluorescence measurements indicated that FITC-intercalated LDH nanoparticles showed a greater degree of energy-dependent uptake rather than passive uptake by BxPC3 cells, especially at high concentrations of nanoparticles. Tetrazolium-based colorimetric assays indicated that BxPC3 cells treated with VP-intercalated LDH nanoparticles showed a significant reduction in cell viability along with about 30-fold reduction in IC_{50} compared to the drug alone. In contrast, the non-drug-intercalated LDH nanoparticles did not affect the cell viability indicating very low innate cytotoxicity. Our research indicates that the superior properties of (Zn, Al)-LDH nanoparticles make them ideal candidates for further development as *in vivo* chemotherapy drug delivery agents.

1. Introduction

Conventional chemotherapeutic strategies involve administration of drugs by oral ingestion or intravenous injection. This typically results in a systemic distribution of the drugs throughout the body with only 10–100 parts per million reaching the desired sites, while the associated secondary effects caused by the rest of the drugs can be serious and sometimes life-threatening. The use of nanocarriers for delivering drugs and imaging agents can significantly improve the pharmacokinetics, biodistribution, cellular uptake, and therapeutic efficacy while lowering the dosage and side effects [1]. An ideal nanocarrier should encapsulate high doses of drugs, remain stable under physiological conditions, protect the drugs from degradation during the transport in the body, and release the drug intracellularly; its surface should remain stable and allow the conjugation of targeting moieties to increase the specificity and effectiveness of being uptaken by cancer cells; after biodegradation, the breakdown products should be biocompatible. In recent years, significant progress has been made in appropriate tailoring of the nanocarrier with/without targeting moieties, and nanocarrier-based therapeutic/imaging agents' delivery has shown great potential for therapy and diagnosis [2–5]. However, diffusion and hydrolysis controlled nanocarrier systems (such as lipid and hydrolytically degradable polymer-based nanoparticles) often release encapsulated agents outside the target tissues, such as in systemic circulation [5, 6]. In general, stability in physiological conditions, controlled release, and stimuli-responsive triggered drug release still remain challenging for nanocarrier development.

Among many nanocarriers (e.g., liposomes, quantum dots, silica spheres, and magnetic nanoparticles), layered double hydroxide (LDH) nanoparticles not only fulfill

many of the aforementioned requirements but also have gained particular attention due to their great flexibility in terms of the chemical compositions, pH-dependent solubility, biocompatibility, and unique anion-intercalating feature [7]. These LDH materials, based on the hydrotalcite $[Mg_6Al_2(OH)_{16}CO_3{\cdot}4H_2O]$ structure, consist of positively charged hydroxide layers with electrostatically held interlayer anions that maintain the charge neutrality. It is well known that the interlayer anions are exchangeable, and the intercalation of a variety of biology-relevant, negatively charged species such as nucleotides, fluorescent dye molecules, DNA, vitamins, acidic drugs has been demonstrated [8–11]. The LDH nanoparticles are usually stable under basic conditions but disintegrate at lower pH (pH of 4-5) found in the lysosome [12] so as to allow the controlled release of intercalated species within the cell. To date, (Mg, Al)-based and (Li, Al)-based LDH nanoparticles have been extensively studied and numerous reports on the synthesis, characterization, and drug delivery have been documented [13–16]. However, several studies related to the drug release profile have reported strong initial bursts. For example, almost 100% Gemfibrozil was released from Gemfibrozil-intercalated $[LiAl_2(OH)_6]$ LDH within 10 minutes at pH 7, [15] and 80% of the intercalated Ibuprofen was released from Ibuprofen-intercalated (Mg, Al)-LDH shortly after 10 minutes at pH 8 [17]. While (Mg, Al)-LDH NPs are still being extensively explored as drug delivery vehicles [18–24], issues related to pH-dependent stability under physiological conditions and temporal drug-release profile along with other questions related to biocompatibility, innate cytotoxicity, and so forth have to be addressed for LDH particles to eventually be successful for therapeutic applications.

In this study, we report the synthesis, characterization, and *in vitro* drug delivery capabilities of LDH nanoparticles based on zinc and aluminum [(Zn, Al)-LDH] as more desirable drug delivery nanocarrier candidates than (Mg, Al)-LDH NPs, which have been ubiquitously reported in the literature. First, we report the synthesis of (Zn, Al)-based LDH NPs and evaluate their pH-dependent stability compared to that of (Mg, Al)-LDH. Next, fluorescein isothiocyanate-(FITC-) intercalated (Zn, Al)-LDH nanoparticles were synthesized and used to study cellular uptake. In order to evaluate the drug delivery capability, valproate- (VP-) intercalated (Zn, Al)-LDH nanoparticles were synthesized and characterized. We also propose the molecular orientation of VP within the LDH, based on the optimized molecular geometry of VP calculated using density functional theory and the interlayer spacing of the VP-intercalated LDH nanoparticles observed using X-ray diffraction (XRD). Finally, *in vitro* cytotoxicity of VP-intercalated (Zn, Al)-LDH nanoparticles on cultured pancreatic cancer cells (BxPC3) was assessed and compared to non-drug-intercalated (Zn, Al)-LDH nanoparticles.

2. Materials and Methods

2.1. Synthesis of (Mg, Al)-LDH and (Zn, Al)-LDH Nanoparticles. $[Mg_{1.85}Al(OH)_2](NO_3){\cdot}xH_2O$ and $[Zn_{2.03}Al(OH)_2](NO_3){\cdot}xH_2O$ nanoparticles, denoted as (Mg, Al, NO_3)-LDH and (Zn, Al, NO_3)-LDH, respectively, were synthesized for the study of the pH-dependent stability using the titration method. The details of the synthesis procedure have been reported elsewhere [25, 26]. Briefly, 10 mL metal salt solution that contains 20 mM of $Zn(NO_3)_2{\cdot}6H_2O$ (or $Mg(NO_3)_2{\cdot}6H_2O$) and $Al(NO_3)_3{\cdot}9H_2O$, with Zn (or Mg) to Al molar ratio of 2, and 10 mL of 40 mM NaOH solution were simultaneously added into a 3-neck flask under nitrogen atmosphere and vigorously stirred (3000 rpm) during the coprecipitation process. Following the constant pH synthesis route, the pH was maintained and the final pH values of the mixture were 5. 98 ± 0.2 for (Zn, Al, NO_3)-LDH and 9 ± 0.2 for (Mg, Al, NO_3)-LDH. Following hydrothermal treatment at 85°C for 3 h, the mixtures were cooled to room temperature and (Zn, Al, NO_3)-LDH/(Mg, Al, NO_3)-LDH nanoparticles were recovered by centrifugation.

2.2. Synthesis of FITC-Intercalated (Zn, Al)-LDH Nanoparticles. Fluorescein isothiocyanate (FITC, Sigma-Aldrich, St. Louis, MO) was intercalated into (Zn, Al, NO_3)-LDH nanoparticles by the ion exchange method [27]. First, the pH of a 40 mL solution of 0.833 mM FITC was gradually adjusted to neutral pH using a 0.25 M NaOH solution. With a targeted molar ratio of FITC to Al of around 0.3, an appropriate amount of (Zn, Al, NO_3)-LDH nanoparticles were then dispersed into a 10 mL FITC solution. The mixture was then aged at 50°C for a few hours; this specific temperature was chosen to avoid any instability of (Zn, Al, NO_3)-LDH nanoparticles and to minimize coarsening [25, 26]. After cooling to room temperature, the FITC-intercalated nanoparticles were collected by centrifugation and used for the investigation of cellular uptake mechanisms.

2.3. Intercalation of VP into (Zn, Al)-LDH Nanoparticles by Ion Exchange. Valproate (VP) was intercalated into (Zn, Al, NO_3)-LDH nanoparticles by the ion exchange method using the VP-Na salt. First, (Zn, Al, NO_3)-LDH nanoparticles were dispersed in alcohol to remove any residual water, recovered by centrifugation, and then dried. Next, the recovered nanoparticles were equilibrated in a 1.667 mM VP-Na solution using hydroalcoholic solvent (i.e., $C_2H_5OH : H_2O = 2:3$ by volume) under a nitrogen atmosphere, and the mixture was aged at 50°C for several hours to facilitate intercalation. After cooling, $Zn_{1.91}Al(OH)_6(NO_3)_{0.584-2y}(CO_3)_y(VP)_{0.416}{\cdot}xH_2O$ nanoparticles, denoted as (Zn, Al, VP)-LDH, were separated by centrifugation, washed in ethanol, and dried at 50°C in vacuum.

2.4. Optimization of VP Molecular Geometry by Computational Study. The optimization of the geometry of VP was carried out using density functional theory. Spin-unrestricted B3LYP method combined with 6-31G* basis set, as provided in the Gaussian 03 package, was used. The molecular orientation of the intercalated VP within the LDH nanoparticles was proposed based on the optimized molecular geometry of VP and the observed interlayer spacing of VP-intercalated LDH nanoparticles by XRD.

2.5. Physicochemical Characterization of LDH Nanoparticles. The morphology and particle size of LDH nanoparticles were examined by bright field transmission electron microscopy (TEM; Philips CM200 with an electron acceleration voltage of 200 kV). The zeta (ζ) potential was determined using a zeta potential analyzer (PSS-NICOMP 380 with zeta potential capability). The crystalline phase information was obtained by powder X-ray diffraction (XRD; Rigaku D/Max-IIB instrument with Cu-K_α radiation, $\lambda = 0.154059$ nm). The loading capacity of VP in (Zn, Al, VP)-LDH nanoparticles was calculated from the total carbon content, determined using a total organic carbon analyzer (Shimadzu TOC-VC/TN). Note that despite the meticulous synthesis conditions, there were some minor CO_3^{2-} contaminants detected in the XRD patterns of (Zn, Al, VP)-LDH nanoparticles, which also contributed to the total carbon content. The elemental compositions of the LDH nanoparticles were determined by inductively coupled plasma atomic emission spectroscopy (ICP; iCAP 6300 ICP Spectrometer).

2.6. Studies of pH-Dependent Aqueous Stability of (Mg, Al, NO_3)-LDH and (Zn, Al, NO_3)-LDH Nanoparticles. Titration experiments were used to study the pH-dependent stability of LDH nanoparticles. First, given amounts of (Mg, Al, NO_3)-LDH and (Zn, Al, NO_3)-LDH nanoparticles were dispersed in deionized water. A 0.1 M HNO_3 solution was then added dropwise into the LDH NPs suspension at an addition rate of 0.1 mL per every 15 min while stirring. The changes of pH were monitored using a pH meter (Fisher Scientific Accumet Excel XL60).

2.7. Cell Culture. The human pancreatic adenocarcinoma cell line, BxPC3, was obtained from ATCC CRL-1687. Cells were cultured in an incubator at 37°C, high humidity, and 5% CO_2 in RPMI-1640 medium (Thermo Fisher Scientific, Waltham, MA) supplemented with 10% FBS (Fisherbrand Research Grade Serum, Thermo Fisher Scientific) and 0.2% penicillin-streptomycin (Cambrex Bio Science, Walkersville, MD). The cells were passaged by trypsinization using standard cell culture protocols. All experiments were performed on cells between passage numbers 18 and 29, and cell counts were determined using a Muse Cell Analyzer (EMD Millipore, Billerica, MA).

2.8. Fluorescence Analysis to Determine Energy-Dependent Cellular Uptake of Nanoparticles. BxPC3 cells were cultured in two 96-well tissue culture plates with 15000 cells per well for 24 h. Prior to the treatment with nanoparticles, one plate was preincubated for 1 hour at 4°C (to determine passive uptake), while the other plate was maintained at 37°C (to determine active uptake). Cells were treated for 1 hour with various concentrations of FITC-intercalated (Zn, Al)-LDH nanoparticles, which were also preincubated for 1 hour at either 4°C or 37°C. After incubation, the media with nanoparticles were removed and the cells were washed with PBS buffer (also preincubated at 4°C or at 37°C). The cells were then lysed by the addition of 100 μL/well of Pierce RIPA lysis buffer (Thermo Fisher Scientific). Fluorescence from the cell lysates was measured at $\lambda_{ex} = 485$ nm and $\lambda_{em} = 520$ nm using the BioTek Synergy 2-plate reader (BioTek, Winooski, VT).

2.9. Dose Response of BxPC3 to Valproate-Sodium (VP-Na) and Determination of IC_{50}. BxPC3 cells were seeded in a 96-well tissue culture plate with 6000 cells per well and incubated for 24 hours. The cell culture media were replaced with media containing various concentrations of VP-Na. After 72 hours, the viability of the cells was assessed using the XTT cell viability assay kit (Gaithersburg, MD) according to the manufacturer's instructions. The cleavage of XTT (a yellow tetrazolium salt) by cells leads to the formation of an orange formazan dye which was quantified by measuring the absorbance at 490 nm in a BioTek Synergy 2-plate reader. All experiments were performed at least three times with quadruple replicates for each treatment. GraphPad Prism software was used to generate a dose response curve and determine IC_{50} of VP-Na for BxPC3 cells.

2.10. Effects of VP-Intercalated (Zn, Al)-LDH Nanoparticles. BxPC3 cells were seeded in a 96-well tissue culture plate with 6000 cells per well and incubated for 24 hours. The cell culture media in the microtiter plate were replaced with media containing various concentrations of VP-intercalated (Zn, Al)-LDH nanoparticles. Media containing (Zn, Al)-LDH nanoparticles intercalated with chloride or nitrate or carbonate anions were used as the controls to assess the effects of the non-drug-intercalated nanoparticles. After 72 hours, the viability of the cells was assessed using the XTT cell viability assay, as described in Section 2.9.

3. Results and Discussion

3.1. Aqueous Stability Study and Suitability of (Mg, Al, NO_3)-LDH and (Zn, Al, NO_3)-LDH Nanoparticles. The particle size and surface charge of nanoparticles can strongly influence the pharmacokinetics, biodistributions, and cellular uptake mechanisms [1]. Moreover, their aqueous stability usually differs significantly from that of bulk materials due to the higher chemical potential that is dictated by interfacial tension and particle size [28]. To ensure that (Mg, Al, NO_3)-LDH and (Zn, Al, NO_3)-LDH nanoparticles used for the aqueous stability study are suitable for biomedicine, TEM was first used to characterize the morphology and particle size. As shown in Figures 1(a) and 1(b), the particle sizes of (Mg, Al, NO_3)-LDH nanoparticles are about 30–50 nm and the sizes of (Zn, Al, NO_3)-LDH nanoparticles, synthesized under the identical conditions, are larger and vary from 200 to 300 nm. Additionally, the positive ζ potential of both types of such discoidal LDH nanoparticles, that is, +48.53 mV for (Zn, Al, NO_3)-LDH and +44.82 mV for (Mg, Al, NO_3)-LDH, indicates that their surface charge may favor the cellular uptake.

XRD was used to identify the intercalated anionic species, and the overall elemental compositions were determined by ICP. Figure 1(c) shows that the experimentally determined d_{003} spacing of both LDH nanoparticles is 8.8 Å ($2\theta = 10°$). With the published data on the thickness of Brucite layer

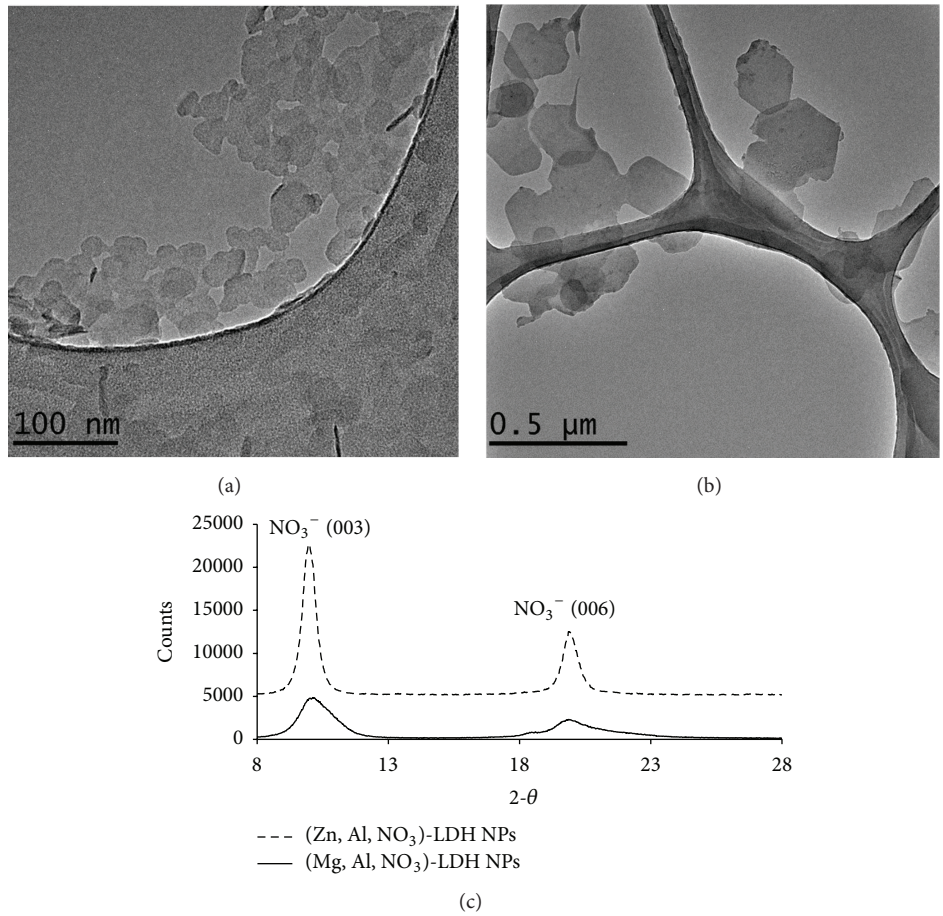

Figure 1: TEM bright field images of (Mg, Al, NO_3)-LDH nanoparticles and (Zn, Al, NO_3)-LDH nanoparticles. The X-ray diffraction patterns of the nanoparticles are shown in (c).

of ~4.8 Å, the gallery spacing was found to be ~4 Å, which verifies that NO_3^- was the only intercalated species in both. However, the relative intensities of their XRD patterns are indicative of the higher crystallinity of (Zn, Al, NO_3)-LDH over (Mg, Al, NO_3)-LDH nanoparticles. Differences in the crystallinity may be attributed to the fact that $Zn(OH)_2$ can fit together well enough to form a more stable crystalline phase than $Mg(OH)_2$ as well as the size differences between the two nanoparticles. Since Boclair et al. reported that cation compositions can greatly influence the formation pH of LDH materials [29, 30], it is expected that the aqueous stability will also be influenced.

The aqueous stability studies of (Mg, Al, NO_3)-LDH and (Zn, Al, NO_3)-LDH nanoparticles at different pH were carried out by the titration method. The pH changes were recorded along with the addition of HNO_3 (0.1 M) titrant and the results are illustrated in Figure 2.

Initially, the pH of deionized water was measured to be 6.76. As soon as (Mg, Al, NO_3)-LDH nanoparticles were dispersed into deionized water, the pH increased from 6.76 and stabilized at 8.91 indicating a rapid and partial dissolution of the nanoparticles. Since K_{sp} (5.61×10^{-12}) of $Mg(OH)_2$ is significantly higher than $Al(OH)_3$ (3×10^{-34}), the released OH^- ions should stem from the ones bonded to Mg^{2+} cations. With the addition of 0.1 M HNO_3 solution, the pH gradually decreased to 5.23 due to partial dissolution of LDH after which the slope of the titration curve remained almost constant until pH of 4.55; the latter is indicative of instability of the crystalline LDH and consequent dissolution at a rapid rate. Further addition of HNO_3 resulted in an immediate drop of pH to a steady state of 2.8. In contrast, after the dispersion of (Zn, Al, NO_3)-LDH nanoparticles into deionized water, the pH decreased from 6.76 and stabilized at 6.15, indicating the weak acidic nature of the surface that can adsorb OH^- anions from the solution. The addition of 0.1 mL of HNO_3 solution instantly dropped the pH to 4.66 after which the pH was maintained upon further addition of HNO_3. This plateau indicates that the rapid dissolution of (Zn, Al, NO_3)-LDH nanoparticles occurred. Further addition of HNO_3 resulted in an immediate drop of pH to a steady state of 2.8.

An ideal LDH nanocarrier composition should have appropriate sensitivity to pH changes, that is, being stable at physiological pH (7.2) during systemic transport but when transfected into a malignant cell and taken up in the lysosome it should release the drug through dissolution [2]. Because of

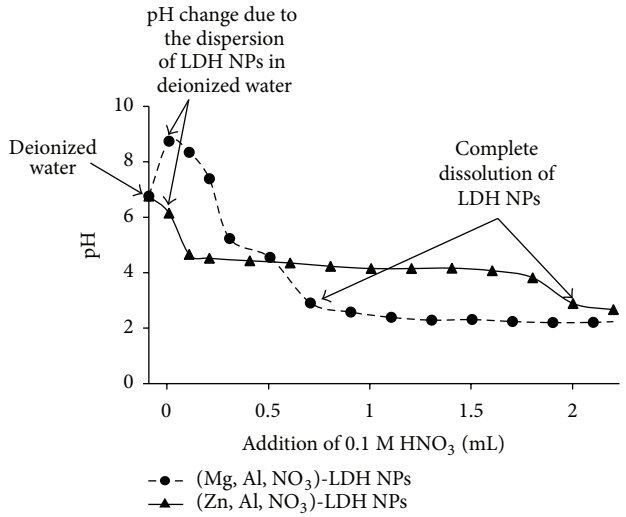

Figure 2: Titration curves to assess the pH-dependent stability of aqueous suspensions of (Mg, Al, NO_3)-LDH and (Zn, Al, NO_3)-LDH nanoparticles using HNO_3 (0.1 M) as the titrant.

site-specific targeting of malignant cells, the LDH nanoparticles will eventually be surface-functionalized with appropriate moieties; this along with the stability characteristics of the LDH will affect the pharmacokinetics, biodistributions, and the cellular uptake mechanisms. The results of the aforementioned aqueous stability studies shed light on the suitability of different cations in LDH-based nanocarriers. For (Mg, Al)-based LDH nanoparticles, a couple of limitations are evident. The observed partial dissolution when dispersed in deionized water would lead to (a) an untimely release of the intercalated drug at physiological pH and (b) the partial or complete loss of surface targeting moieties. In contrast, (Zn, Al)-based LDH nanoparticles have an excellent stability at pH > 5. This implies that (Zn, Al)-based LDH nanoparticles have greater stability at physiological pH and are capable of releasing the drug intracellularly within the lysosome. Additionally, their stable surfaces can form robust covalent bonds with targeting moieties for improved bioavailability and targetability. Moreover, the better crystallinity would facilitate intercalation of negatively charged drugs via ion exchange after synthesis. These factors along with the outstanding biocompatibility (data shown in Section 3.3) make (Zn, Al)-based LDH an ideal composition for incorporating both imaging agent (FITC) and drug (VP) as in the following studies.

3.2. Cellular Uptake of (Zn, Al)-LDH Nanoparticles. The uptake of extracellular materials such as nanoparticles may involve multiple mechanisms. Understanding of the involved mechanisms in the cellular uptake is important since the intracellular fate is usually linked to the mechanism of entry. The various molecular pathways for uptake of nanoparticles can be broadly divided into those that require energy (active uptake) or those that do not require energy (passive uptake). In order to determine if the uptake of nanoparticles was an active or passive process, FITC-intercalated LDH nanoparticles were used for the study. $Zn_{2.03}Al(OH)_6(FITC)_xCl_{1-x}{\cdot}yH_2O$ nanoparticles with $x \approx 0.15$, denoted as (Zn, Al, FITC)-LDH, were prepared according to the procedures described in the experimental section. The bright field TEM micrograph for (Zn, Al, FITC)-LDH is shown in Figure 3(a). The successful intercalation of FITC was validated by XRD studies (Figure 3(b)). Note that, during the preparation of the FITC solution for intercalation, deprotonation of FITC was monitored using a pH electrode filled with a saturated KCl solution, which led to the replacement of the intercalated NO_3^- by Cl^- ions. While the primary XRD peaks at 2θ of 11.47° (d_{003} = 7.7 Å) and 23.4° (d_{006} = 3.8 Å) correspond to the intercalated Cl^- anion, the extra hump centered at 2θ of 5.18° is indicative of an expansion (d_{003} = 17.05 Å) due to the presence of the intercalated FITC. Also by subtracting the double hydroxide layer thickness of about 4.8 Å [31], an interlayer gallery spacing of ~12.25 Å corresponds to the size of the intercalated FITC.

Cell cultures incubated at either 37°C (normal cell culture temperature) or 4°C (lower temperature) were treated with (Zn, Al, FITC)-LDH. Since energy-dependent pathways tend to be inhibited at lower temperatures, this allowed us to assess the energy dependence on the cellular uptake of nanoparticles. Relative fluorescence measured from cells (Figure 4) shows that the uptake of nanoparticles involves a combination of both active and passive processes. However, at higher concentrations (5 mM), there appears to be a greater dependence (about 50% higher) on energy-mediated pathways for the entry of the nanoparticles into the cell.

Several other studies have utilized endocytosis inhibitors such as genistein, chlorpromazine, and nocodazole to investigate the specific active pathways involved in the cellular uptake of nanoparticles. We were not able to clearly distinguish between the different endocytosis pathways for the uptake of (Zn, Al, FITC)-LDH nanoparticles using these inhibitors (data not shown). Several other reports have also indicated ambiguity with their uptake data while using these inhibitors [32].

3.3. Effect of VP on Cultured Pancreatic Cancer BxPC3 Cells. Valproic acid (VPA, 2-propylpetanoic acid) is a short chain fatty acid that has been approved by the FDA for the treatment of epilepsy, bipolar disorders, and migraine and has been clinically used for schizophrenia. More recently there has been an interest in VPA as an anticancer drug and it is currently being assessed in clinical trials for the treatment of different tumors [33]. While the molecular mechanisms by which VPA can act as anticancer drug are not fully understood, its ability to inhibit histone deacetylases and activate notch-1 signaling seems to be important [34]. The ability of VPA to inhibit the proliferation of cultured pancreatic cancer cells is particularly interesting since this is a deadly disease with an extremely high rate of mortality. When we tested the antiproliferative effects of VP-Na on the cultured human pancreatic adenocarcinoma cell line BxPC3, we found that it is effective at high concentrations (IC_{50} of 63.21 mM, Figure 5). Other studies have shown that this effect

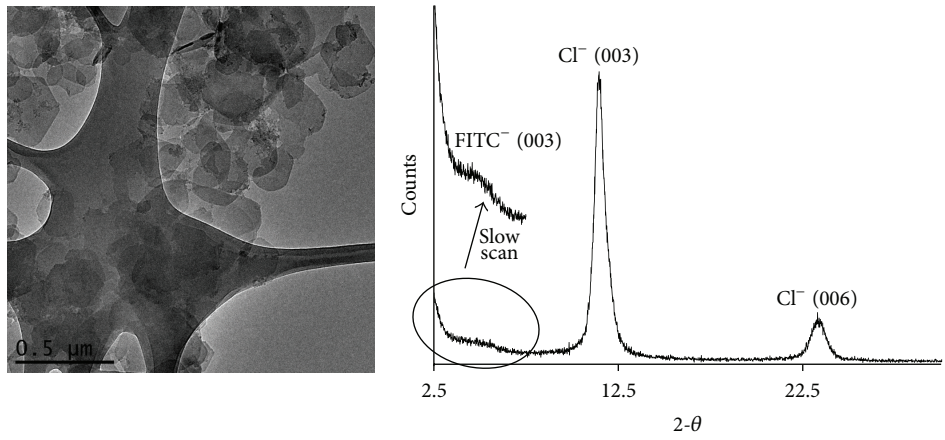

Figure 3: TEM bright field micrograph of $Zn_2Al(OH)_6(FITC)_xCl_{1-x}{\cdot}xH_2O$, $x \approx 0.15$, in (a); the corresponding XRD pattern is shown in (b), with a slow scan at 2-θ between 2.5 and 7.5.

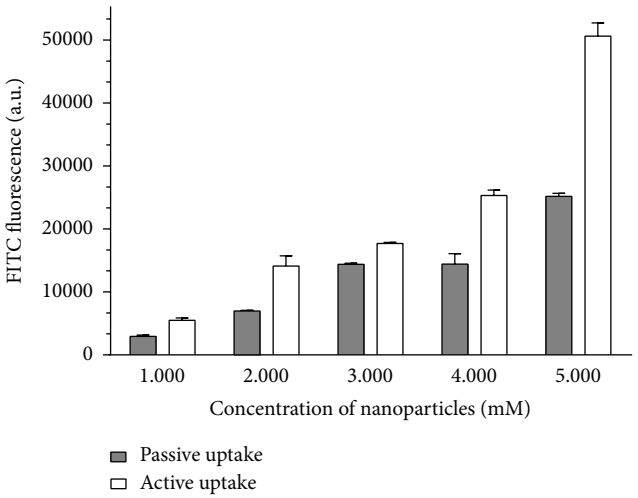

Figure 4: Assessment of energy dependence of the uptake of nanoparticles. Fluorescence from BxPC3 cell treated with (Zn, Al, FITC)-LDH nanoparticles at either 37°C (active uptake) or at 4°C (passive uptake). x-axis represents the concentration of the nanoparticles in terms of Al content.

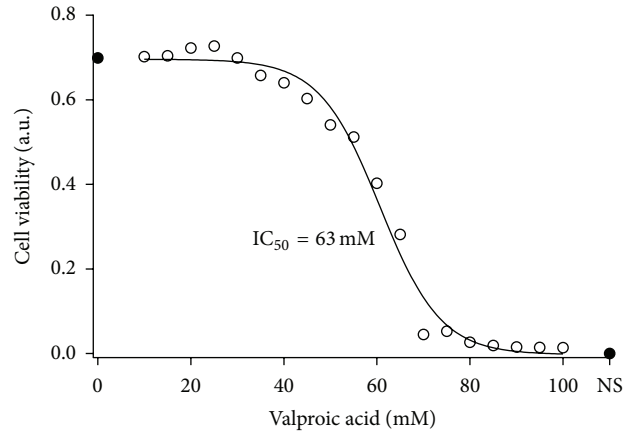

Figure 5: Dose response of the viability of BxPC3 cells to various concentrations of valproate-sodium to determine IC_{50} of the drug. Note that (Zn, Al)-LDH nanoparticles were not used for drug delivery for this experiment.

is primarily due to the downregulation of the Alzheimer amyloid precursor protein [35].

Meanwhile the high IC_{50} *in vitro* on cultured cells indicates that a very high dose is required *in vivo* for effective chemotherapy. This is a cause for concern since the drug has a high risk of side effects, especially due to its psychoactive properties. A promising strategy to overcome this challenge and improve the therapeutic index of such drugs is the use of LDH nanoparticles for drug delivery. Hence, for this study, we utilized VP for proof-of-concept experiments to demonstrate the utility of (Zn, Al)-LDH nanoparticles for drug delivery to cultured pancreatic cancer BxPC3 cells.

3.4. Characterization of VP-Intercalated (Zn, Al)-LDH Nanoparticles. Valproate-intercalated (Zn, Al)-LDH nanoparticles were synthesized and *in vitro* toxicity studies were carried out using pancreatic cancer cells, and the results were compared to using Na-VP alone. The long hydrophobic tail of VP was originally designed to balance the partition coefficient and increase the lipophilicity and the penetration into the cell. However, it was found that, in aqueous medium, VP self-organize to form micelles, which could partially dissolve LDH materials by capturing the metal ions. Consequently, it was necessary to use an alcohol-aqueous solution to attain a higher solubility of VP during ion exchange and thereby prevent the formation of micelles and dissolution of the LDH nanoparticles. ζ potential of (Zn, Al, NO_3)-LDH nanoparticles was measured to be 48.53 mV, but, after the intercalation of VP, ζ potential of

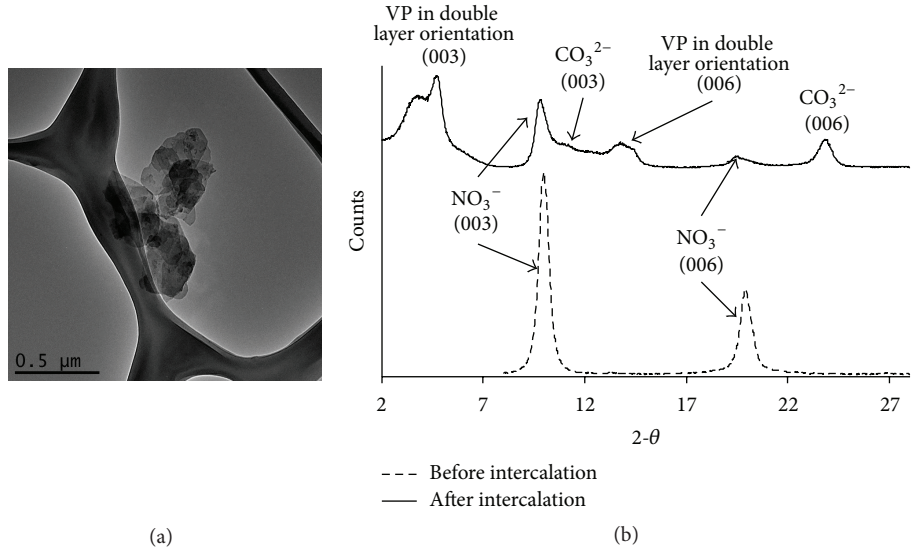

Figure 6: TEM bright field micrograph of $Zn_{1.91}Al(OH)_6(NO_3,0.5CO_3)_{0.584}(VP)_{0.416}{\cdot}xH_2O$ nanoparticles is shown in (a), and XRD analysis before and after intercalation shown in (b) shows the partial replacement of the intercalated NO_3^- by VP and CO_3^{2-} (as minor contaminants).

$Zn_{1.91}Al(OH)_6(NO_3)_{0.584-2y}(CO_3)_y(VP)_{0.416}{\cdot}xH_2O$ (hereon denoted as (Zn, Al, VP)-LDH) nanoparticles decreased to 37 mV, indicating that some surface adsorption of VP had occurred. The TEM micrograph in Figure 6(a) shows that the particle size of (Zn, Al, VP)-LDH NPs is ~350–500 nm, formed due to minor agglomeration of primary nanoparticles (~150 nm) due to lowered ζ potential. The XRD patterns before and after the intercalation, shown in Figure 6(b), validate the successful intercalation of VP, with some minor contamination of the intercalated CO_3^{2-}. The significant expansion of the interlayer spacing occurred due to the intercalation of VP, and the observation of two peaks at 2θ of 3.74° and 4.72° suggests that intercalated VP can exist in two different forms. By assuming a thickness of the double hydroxide layer to be ~4.80 Å [31], the interlayer spacings are then 18.8 Å and 13.9 Å, respectively.

To determine the molecular orientation of the intercalated VP that gives rise to these interlayer spacings, the geometry of VP was first optimized by the spin-unrestricted B3YLP method, using diffuse function basis set of 6-31G*, and the optimized geometry is illustrated in Figure 7(a). The data suggests that VP is intercalated in double layer orientation, but, as depicted in Figure 7(b), the hydration levels may vary.

3.5. Delivery of Valproate to Pancreatic Cancer BXPC3 Cells Using Valproate-Intercalated (Zn, Al)-LDH Nanoparticles. In order to assess the utility of the newly synthesized (Zn, Al)-LDH nanoparticles for drug delivery, cultured pancreatic cancer BxPC3 cells were treated with VP-intercalated LDH nanoparticles. It appears that the drug-intercalated nanoparticles are stable in cell culture media and can be efficiently uptaken by the cells leading to delivery of large doses of the drug. While the positive surface charge of (Zn, Al, VP)-LDH nanoparticles may provide excellent affinity to the cell surface, the exact molecular mechanism for the uptake of the LDH nanoparticles into the cell was not determined in this study. A significant reduction in the amount of VP required to lower cell viability was observed when the drug was delivered using the nanoparticles, leading to an approximately 30-fold reduction in IC_{50} from 63.21 mM to about 2 mM in pancreatic cancer BxPC3 cells.

(Zn, Al)-LDH nanoparticles intercalated with carbonate (Zn, Al, CO_3) or chloride (Zn, Al, Cl) or nitrate (Zn, Al, NO_3) anions were used as the controls to study the effect of nanoparticles without the drug on the cancer cells. The corresponding XRD and TEM micrographs are shown in Figure S1 in Supplementary Material available online at http://dx.doi.org/10.1155/2015/350370. Figure 8 shows the effects of (Zn, Al, VP)-LDH nanoparticles along with the control nanoparticles on BxPC3 cells. The control nanoparticles did not significantly lower the viability of BxPC3 cells in the range of concentrations tested. The lack of cytotoxicity may be due to the fact that (Zn, Al)-LDH nanoparticles are synthesized from inorganic ions which are not toxic to human cells at low concentrations. The excellent biocompatibility indicates that any side effects due to the nanoparticle itself are likely to be minimum when it is used *in vivo*.

The high stability, excellent biocompatibility, and superior *in vitro* drug delivery properties of (Zn, Al)-LDH nanoparticles show promise that these nanoparticles may retain their *in vivo* efficacy. In this study, VP was used as proof-of-concept to demonstrate the utility of (Zn, Al)-LDH nanoparticles for drug delivery. While VP may not prove to be the ideal drug for cancer therapy, our results indicate that (Zn, Al)-LDH nanoparticles have great potential for the delivery of various chemotherapeutic agents. Further modification of (Zn, Al)-LDH nanoparticles to include cancer cell targeting ligands on the surface is likely to enhance drug delivery and further minimize off-target effects.

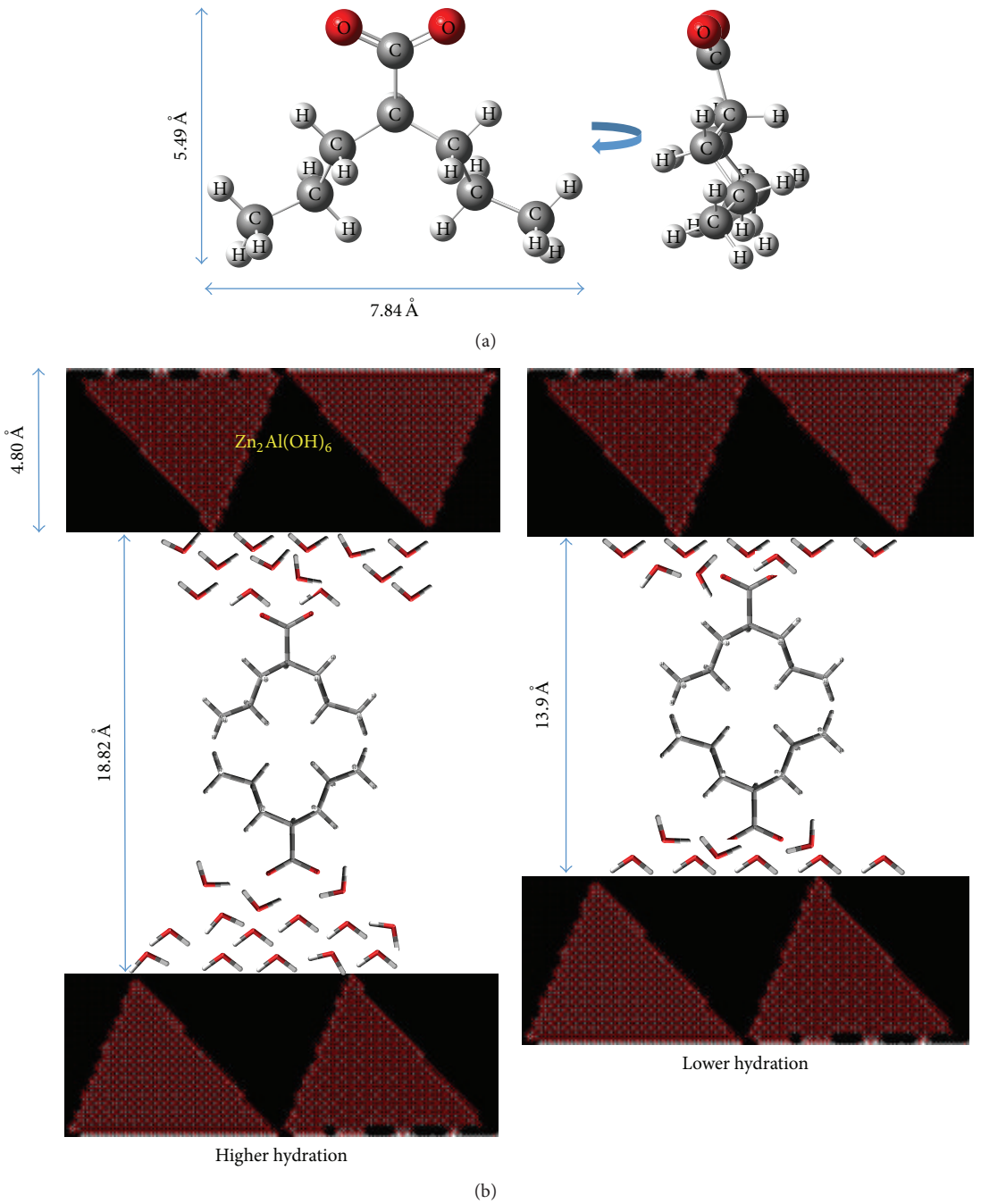

FIGURE 7: (a) shows GaussView 03 generated 3D representation of the optimized geometry of VP by spin unrestricted B3YLP method using 6-31G* basis set. In (b), the intercalated VP are proposed to be in double layer orientation with different hydration levels according to the interlayer spacing calculated from XRD pattern and the optimized geometry of the VP.

4. Conclusions

In this study, it was found that (Zn, Al)-LDH nanoparticles have excellent physicochemical properties as ideal nanocarriers for pH-sensitive drug delivery. In comparison to (Zn, Al)-LDH nanoparticles, (Mg, Al)-LDH nanoparticles were observed to have poor stability at pH lower than 8.91. This may, in part, explain the rapid release of the intercalated drugs under physiological conditions (pH ~7.2) from (Mg, Al)-LDH nanoparticles. In contrast, (Zn, Al)-based LDH nanoparticles showed an excellent stability above pH 4.66, which may indicate greater stability under physiological conditions leading to selective release of the drug upon reaching the lysosomes within cells. Such a greater stability also

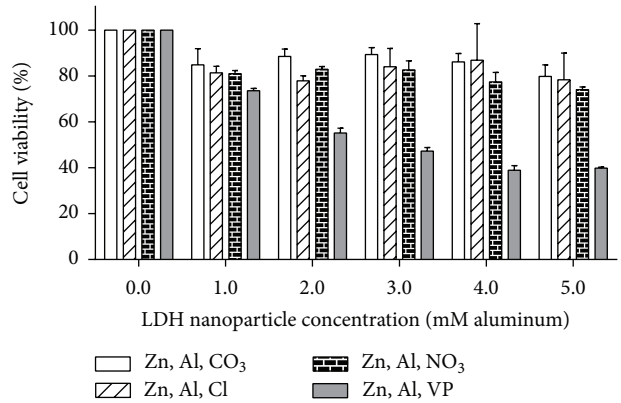

Figure 8: The effect of (Zn, Al)-LDH nanoparticles intercalated with valproate (Zn, Al, VP) on the viability of cultured pancreatic cancer BXPC3 cells. The effect of nanoparticles without the drug was assessed by using (Zn, Al)-LDH nanoparticles intercalated with either carbonate (Zn, Al, CO_3), chloride (Zn, Al, Cl), or nitrate (Zn, Al, NO_3) anions.

makes them better candidates for targeted drug delivery by incorporating cell targeting ligands onto the surface. The use of (Zn, Al, FITC)-LDH nanoparticles revealed that energy-dependent cellular uptake mechanisms are more active at higher nanoparticle concentrations. When the ability of (Zn, Al)-LDH nanoparticles to deliver VP into pancreatic cancer BxPC3 cells was tested, we found a 30-fold reduction in IC_{50} value of VP. In addition to their excellent drug delivery capabilities, (Zn, Al)-based LDH nanoparticles were also found to be highly biocompatible since control nanoparticles (without drug intercalation) were found to have minimal cytotoxicity.

Although VP was used as proof-of-concept to demonstrate the utility of (Zn, Al)-LDH nanoparticles for drug delivery, results from the current work indicate that these nanoparticles have excellent utility for the delivery of several other chemotherapeutic agents. In addition, the ability of (Zn, Al)-LDH nanoparticles to intercalate and deliver magnetic resonance imaging contrast agents makes them suitable for theranostic applications. The biocompatibility and *in vivo* utility of (Zn, Al)-LDH nanoparticles for drug delivery will have to be tested in animal models to assess the potential for ultimate use in patients.

Conflict of Interests

The authors declare that there is no conflict of interests regarding the publication of this paper.

Acknowledgments

Sandwip K. Dey acknowledges financial support from the National Cancer Institute, National Institutes of Health (1R21CA133618), National Science Foundation (CBET-0829128), and ASU Foundation's Women & Philanthropy program (WZ91010). The authors gratefully acknowledge the use of facilities within the LeRoy Eyring Center for Solid State Science at Arizona State University and are grateful to Dr. Thomas Groy, Dr. Robert Wang, and Dr. Karl Weiss of ASU for assistance with XRD, DLS, and TEM. The authors thank Bernardo Chavira and Zachary Emmons for technical help.

References

[1] S. M. Moghimi, A. C. Hunter, and J. C. Murray, "Long-circulating and target-specific nanoparticles: theory to practice," *Pharmacological Reviews*, vol. 53, no. 2, pp. 283–318, 2001.

[2] J.-M. Oh, S.-J. Choi, S.-T. Kim, and J.-H. Choy, "Cellular uptake mechanism of an inorganic nanovehicle and its drug conjugates: enhanced efficacy due to clathrin-mediated endocytosis," *Bioconjugate Chemistry*, vol. 17, no. 6, pp. 1411–1417, 2006.

[3] T. Tanaka, P. Decuzzi, M. Cristofanilli et al., "Nanotechnology for breast cancer therapy," *Biomedical Microdevices*, vol. 11, no. 1, pp. 49–63, 2009.

[4] J. Xie, S. Lee, and X. Chen, "Nanoparticle-based theranostic agents," *Advanced Drug Delivery Reviews*, vol. 62, no. 11, pp. 1064–1079, 2010.

[5] E. Cukierman and D. R. Khan, "The benefits and challenges associated with the use of drug delivery systems in cancer therapy," *Biochemical Pharmacology*, vol. 80, no. 5, pp. 762–770, 2010.

[6] M. Caldorera-Moore, N. Guimard, L. Shi, and K. Roy, "Designer nanoparticles: incorporating size, shape and triggered release into nanoscale drug carriers," *Expert Opinion on Drug Delivery*, vol. 7, no. 4, pp. 479–495, 2010.

[7] Z. P. Xu and G. Q. Lu, "Layered double hydroxide nanomaterials as potential cellular drug delivery agents," *Pure and Applied Chemistry*, vol. 78, no. 9, pp. 1771–1779, 2006.

[8] M. S. Gasser, "Inorganic layered double hydroxides as ascorbic acid (vitamin C) delivery system-Intercalation and their controlled release properties," *Colloids and Surfaces B: Biointerfaces*, vol. 73, no. 1, pp. 103–109, 2009.

[9] H. Nakayama, A. Hatakeyama, and M. Tsuhako, "Encapsulation of nucleotides and DNA into Mg-Al layered double hydroxide," *International Journal of Pharmaceutics*, vol. 393, no. 1-2, pp. 104–111, 2010.

[10] V. Rives, M. del Arco, and C. Martín, "Intercalation of drugs in layered double hydroxides and their controlled release: a review," *Applied Clay Science*, vol. 88-89, pp. 239–269, 2014.

[11] A. W. Musumeci, Z. P. Xu, S. V. Smith, R. F. Minchin, and D. J. Martin, "Layered double hydroxide nanoparticles incorporating terbium: Applicability as a fluorescent probe and morphology modifier," *Journal of Nanoparticle Research*, vol. 12, no. 1, pp. 111–120, 2010.

[12] N. Fehrenbacher and M. Jäättelä, "Lysosomes as targets for cancer therapy," *Cancer Research*, vol. 65, no. 8, pp. 2993–2995, 2005.

[13] V. Ambrogi, G. Fardella, G. Grandolini, and L. Perioli, "Intercalation compounds of hydrotalcite-like anionic clays with antiinflammatory agents—I. Intercalation and in vitro release of ibuprofen," *International Journal of Pharmaceutics*, vol. 220, no. 1-2, pp. 23–32, 2001.

[14] A. I. Khan, L. X. Lei, A. J. Norquist, and D. O'Hare, "Intercalation and controlled release of pharmaceutically active compounds from a layered double hydroxide," *Chemical Communications*, no. 22, pp. 2342–2343, 2001.

[15] A. I. Khan and D. O'Hare, "Intercalation chemistry of layered double hydroxides: recent developments and applications," *Journal of Materials Chemistry*, vol. 12, no. 11, pp. 3191–3198, 2002.

[16] S. Carlino, "The intercalation of carboxylic acids into layered double hydroxides: a critical evaluation and review of the different methods," *Solid State Ionics*, vol. 98, no. 1-2, pp. 73–84, 1997.

[17] B. Li, J. He, D. G. Evans, and X. Duan, "Inorganic layered double hydroxides as a drug delivery system—intercalation and in vitro release of fenbufen," *Applied Clay Science*, vol. 27, no. 3-4, pp. 199–207, 2004.

[18] K. Zhang, Z. P. Xu, J. Lu et al., "Potential for layered double hydroxides-based, innovative drug delivery systems," *International Journal of Molecular Sciences*, vol. 15, no. 5, pp. 7409–7428, 2014.

[19] G. Choi, S. Y. Kim, J.-M. Oh, and J.-H. Choy, "Drug-ceramic 2-dimensional nanoassemblies for drug delivery system in physiological condition," *Journal of the American Ceramic Society*, vol. 95, no. 9, pp. 2758–2765, 2012.

[20] Y. Y. Wong, H. M. Cooper, K. Zhang, M. Chen, P. Bartlett, and Z. P. Xu, "Efficiency of layered double hydroxide nanoparticle-mediated delivery of siRNA is determined by nucleotide sequence," *Journal of Colloid and Interface Science*, vol. 369, no. 1, pp. 453–459, 2012.

[21] K. Ladewig, M. Niebert, Z. P. Xu, P. P. Gray, and G. Q. M. Lu, "Efficient siRNA delivery to mammalian cells using layered double hydroxide nanoparticles," *Biomaterials*, vol. 31, no. 7, pp. 1821–1829, 2010.

[22] M. Chen, H. M. Cooper, J. Z. Zhou, P. F. Bartlett, and Z. P. Xu, "Reduction in the size of layered double hydroxide nanoparticles enhances the efficiency of siRNA delivery," *Journal of Colloid and Interface Science*, vol. 390, no. 1, pp. 275–281, 2013.

[23] M. Herrero, F. M. Labajos, and V. Rives, "Size control and optimisation of intercalated layered double hydroxides," *Applied Clay Science*, vol. 42, no. 3-4, pp. 510–518, 2009.

[24] Z. Gu, B. E. Rolfe, Z. P. Xu, J. H. Campbell, G. Q. M. Lu, and A. C. Thomas, "Antibody-targeted drug delivery to injured arteries using layered double hydroxide nanoparticles," *Advanced Healthcare Materials*, vol. 1, no. 5, pp. 669–673, 2012.

[25] X. Sun, E. Neuperger, and S. K. Dey, "Insights into the synthesis of layered double hydroxide (LDH) nanoparticles: part 1. Optimization and controlled synthesis of chloride-intercalated LDH," *Journal of Colloid and Interface Science*, vol. 459, pp. 264–272, 2015.

[26] X. Sun and S. K. Dey, "Insights into the synthesis of layered double hydroxide (LDH) nanoparticles: part 2. Formation mechanisms of LDH," *Journal of Colloid and Interface Science*, vol. 458, pp. 160–168, 2015.

[27] L. Perioli, T. Posati, M. Nocchetti, F. Bellezza, U. Costantino, and A. Cipiciani, "Intercalation and release of antiinflammatory drug diclofenac into nanosized ZnAl hydrotalcite-like compound," *Applied Clay Science*, vol. 53, no. 3, pp. 374–378, 2011.

[28] P. W. Schindle, "Heterogeneous equilibria involving oxides, hydroxides, carbonates, and hydroxide carbonates," in *Equilibrium Concepts in Natural Water Systems*, vol. 67 of *Advances in Chemistry Series*, chapter 9, pp. 196–221, American Chemical Society, 1967.

[29] J. W. Boclair and P. S. Braterman, "Layered double hydroxide stability. 1. Relative stabilities of layered double hydroxides and their simple counterparts," *Chemistry of Materials*, vol. 11, no. 2, pp. 298–302, 1999.

[30] J. W. Boclair, P. S. Braterman, J. P. Jiang, S. W. Lou, and F. Yarberry, "Layered double hydroxide stability. 2. Formation of Cr(III)-containing layered double hydroxides directly from solution," *Chemistry of Materials*, vol. 11, no. 2, pp. 303–307, 1999.

[31] R. Allmann, "The crystal structure of pyroaurite," *Acta Crystallographica Section B: Structural Crystallography and Crystal Chemistry*, vol. 24, pp. 972–977, 1968.

[32] I. A. Khalil, K. Kogure, H. Akita, and H. Harashima, "Uptake pathways and subsequent intracellular trafficking in nonviral gene delivery," *Pharmacological Reviews*, vol. 58, no. 1, pp. 32–45, 2006.

[33] M. Michaelis, H. W. Doerr, and J. Cinatl Jr., "Valproic acid as anti-cancer drug," *Current Pharmaceutical Design*, vol. 13, no. 33, pp. 3378–3393, 2007.

[34] D. Y. Greenblatt, A. M. Vaccaro, R. Jaskula-Sztul et al., "Valproic acid activates Notch-1 signaling and regulates the neuroendocrine phenotype in carcinoid cancer cells," *Oncologist*, vol. 12, no. 8, pp. 942–951, 2007.

[35] V. Venkataramani, C. Rossner, L. Iffland et al., "Histone deacetylase inhibitor valproic acid inhibits cancer cell proliferation via down-regulation of the alzheimer amyloid precursor protein," *The Journal of Biological Chemistry*, vol. 285, no. 14, pp. 10678–10689, 2010.

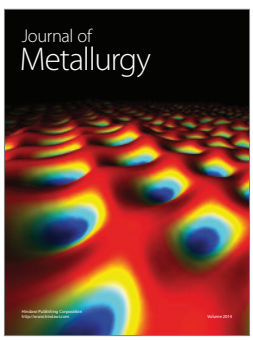

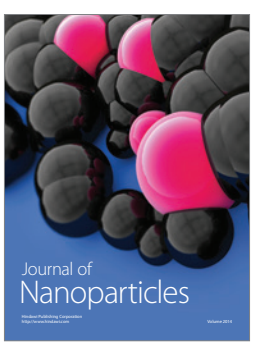

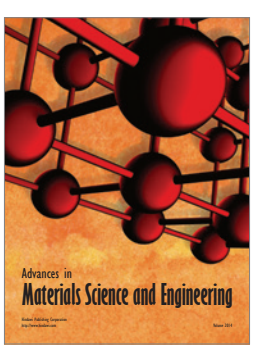

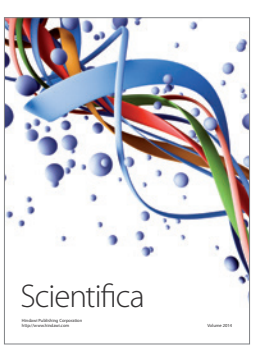

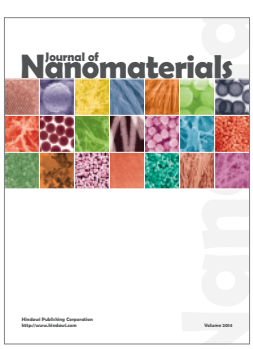

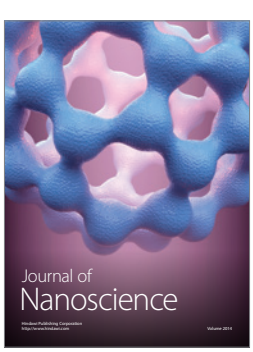

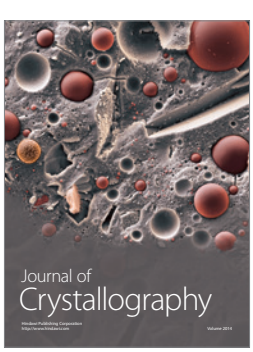

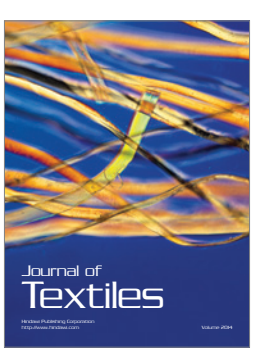

Hindawi

Submit your manuscripts at
http://www.hindawi.com